Supporting Information

Heterozygous mutation in *BRCA2* induces accelerated age-dependent decline in sperm quality with male subfertility in rats

Yashiro Motooka, Hideaki Tanaka, Yuki Maeda, Misako Katabuchi, Tomoji Mashimo, Shinya Toyokuni

Supporting Tables

Table S1. Summary of primers for PCR

Table S2. Summary of the antibodies used in this study

Table S3. Criteria for Johnsen's score

Supporting Figures

Figure S1. Sanger sequencing shows no mutation in the regions of potential off-target effects

Figure S2. Metaphase spermatocytes in *Brca2*$^{wt/mut}$ testes exhibited lower staining intensity for BRCA2 and phosphorylated BRCA2 in immunohistochemistry compared to *Brca2*$^{wt/wt}$

Figure S3. Uncropped images of membranes used for immunoblotting

Figure S4. Immunohistochemistry shows no significant differences in oxidative stress markers, 8-OHdG and 4-HNE, in the testes of *Brca2*$^{wt/mut}$ rat at 11 weeks

Figure S5. Representative images of TUNEL staining for each main stage of seminiferous tubules

Figure S6. Representative plots of SCSA

Table S1. Summary of primers for PCR

Target name	Primer type	Primer name	Target information	The primer sequence from 5' end to 3' end	Length	Tm value	GC content (%)
Brca2 wild type	Forward	*Brca2*-F	Wild type allele	CCAAAGTGTGTCTGGACTGAAG	22	59.8	50
Brca2 wild type	Reverse	*Brca2*-R	Wild type allele	ATTCTGGGGTTCTGCTTTCA	20	59.7	45
Founder No.18 and 27	Forward	*Brca2*-MUT-F	Newly formed nucleotide sequence	CATCCTTCACGCAAGTGG	18	57.6	55.56
Brca2 wild type	Forward	*Brca2*-F2	Nucleotide sequence commonly deleted in this genome editing	CGCACTTATGGAATTTTTAGCAC	23	60	39.1
Founder No3	Forward	*Brca2*-F3d8-F	Newly formed nucleotide sequence	AGGAAGTCCATCCTTCATGG	20	58.5	50
Inframe deletion of Founder No6, 7, 9, and 19	Forward	*Brca2*-F6d18-F	Newly formed nucleotide sequence	ATCCTTCACGCACAGCAAG	19	60	52.63
Founder No6	Forward	*Brca2*-F6d17-F	Newly formed nucleotide sequence	CAGGAAGTCCATCCTTTTTAGC	22	58.4	45.45
Founder No7	Forward	*Brca2*-F7d20a1-F	Newly formed nucleotide sequence	ATCCTTCACGCACACAAG	18	56.9	50
Founder No9	Forward	*Brca2*-F9d50-F	Newly formed nucleotide sequence	GGAAACTTGGGATACATGGAA	21	57.2	42.86
Founder No16	Forward	*Brca2*-F16d299-F	Newly formed nucleotide sequence	TCCATCCTTCACGCACTTAC	20	59.2	50
Inframe deletion of Founder No19	Forward	*Brca2*-F19d18-F	Newly formed nucleotide sequence	TCCATCCTTCACGCAAGTG	19	59.4	52.63
Founder No19	Forward	*Brca2*-F19d50-F	Newly formed nucleotide sequence	GGGATACATGTAATTTTTAGCACAGC	26	60.1	38.46
Founder No24-1	Forward	*Brca2*-F24d9a1-F	Newly formed nucleotide sequence	CATCCTTCACGCACATTTTAGC	22	59.7	45.45
Founder No24-2	Forward	*Brca2*-F24d17-F	Newly formed nucleotide sequence	CAGGAAGTCCAGAATTTTTAGCAC	24	59.4	41.67
Founder No26-1	Forward	*Brca2*-F26d6-F	Newly formed nucleotide sequence	AAGTCCATCCTTCACGTGG	19	58.8	52.63
Founder No26-2	Forward	*Brca2*-F26d13-F	Newly formed nucleotide sequence	CCATCCTTCATTTTTAGCACAGC	23	59.8	43.48
Founder No27	Forward	*Brca2*-F27d23-F	Newly formed nucleotide sequence	TTCACGCAAGTGGAAAAGC	19	58.5	47.37
Off target 1	Forward	Fot1	Possible off target site 1	TAAGAGATGTTCCTTCCACTCCTAATC	27	59.9	40.74
Off target 1	Reverse	Rot1	Possible off target site 1	GCACATGATCAGCATCTACACATC	24	60.0	45.83
Off target 2	Forward	Fot2	Possible off target site 2	CAGATTGGACTGTACTGACCTTGTG	25	61.3	48.00
Off target 2	Reverse	Rot2	Possible off target site 2	GTGTATAGTACAGGGTGTGTTTCAGGAG	28	62.8	46.43

35 **Table S2. Summary of the antibodies used in this study**

36

Target molecule [clone]	Immunized host	Supplier	Ordering Number	Antigen retrieval	Dilution for IHC	Dilution for immunoblotting
BRCA2 (aa 1-100)	Rabbit	abcam	ab216972	ER1 10 min	1:1,000	1:1000
BRCA2 (E2070-S2120)	Rabbit	Invitrogen	PA5-105731	ER1 10 min	1:1,000	1:1000
Phosphorylated BRCA2	Rabbit	Invitrogen	PA5-105585	ER1 10 min	1:1,000	1:1000
DDX4 / MVH [RM1022]	Rabbit	abcam	ab284611	ER1 10 min	1:1,000	
γH2AX [JBW301]	Mouse	Merck	05-636	ER1 10 min	1:500	
8-OHdG [N45.1]	Mouse	In house (26)		ER1 10 min	1:8,000	
4-HNE [HNE-J2]	Mouse	In house (27)		ER1 10 min	1:20,000	
β-actin [AC-15]	Mouse	Sigma-Aldrich	A1978			1:2000

37

38

39 **Table S3. Criteria for Johnsen's score**

40

Johnsen's score	Pathological findings
Score 10	Complete spermatogenesis with spermatozoa. (Spermatozoa are here defined as cells having achieved the small head form of the spermatozoon). Germinal epithelium organized in a regular thickness leaving an open lumen.
Score 9	Many spermatozoa present but germinal epithelium disorganized with marked sloughing or obliteration of lumen.
Score 8	Only few spermatozoa (<5-10) present in section
Score 7	No spermatozoa but many spermatids present.
Score 6	No spermatozoa and only few spermatids (<5-10)) present.
Score 5	No spermatozoa, no spermatid s but several or many spermatocytes present.
Score 4	Only few spermatocytes (<5) and no spermatids or spermatozoa present.
Score 3	Spermatogonia are the only germ cells present.
Score 2	No germ cells but Sertoli cells are present.
Score 1	No cells in tubular section.

41

Figure S1. Sanger sequencing shows no mutation in the regions of potential off-target effects

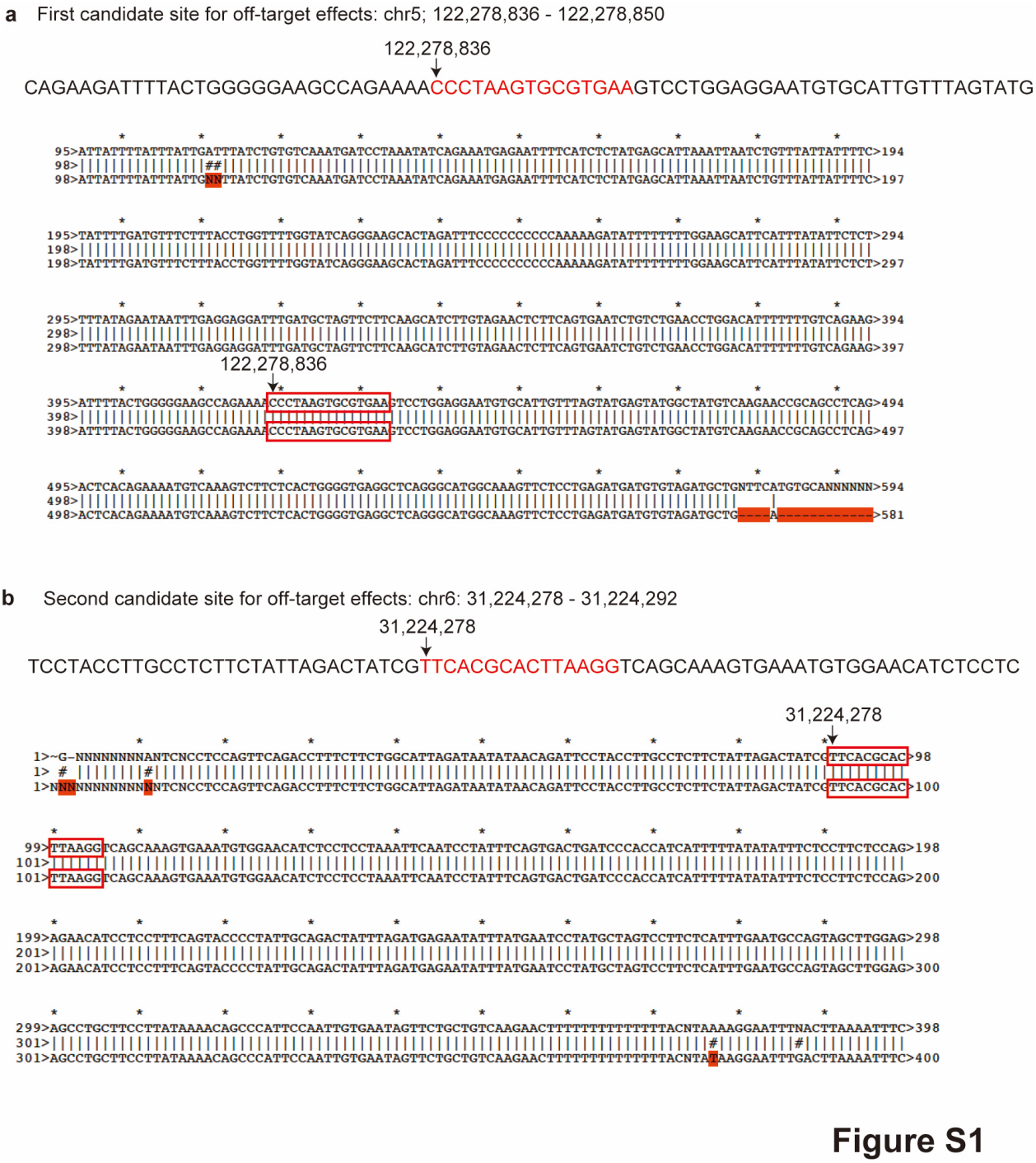

Figure S1. Sanger sequencing shows no mutation in the regions of potential off-target effects

(a, b) Two candidate sites for off-target effects caused by this genome editing, detected by CRISPRdirect, along with the Sanger sequencing results for the surrounding regions of each site. The results of Sanger sequencing are compared with the sequence of the wild-type SD rat. The upper row represents the wild type, and the lower row is from the founder rat with *Brca2* p.T1942Kfs*8 allele. (a) Possible off-target region on chromosome 5. (b) Possible off-target region on chromosome 6.

Figure S2. Metaphase spermatocytes in *Brca2*$^{wt/mut}$ testes exhibits lower staining intensity for BRCA2 and phosphorylated BRCA2 in immunohistochemistry compared to *Brca2*$^{wt/wt}$

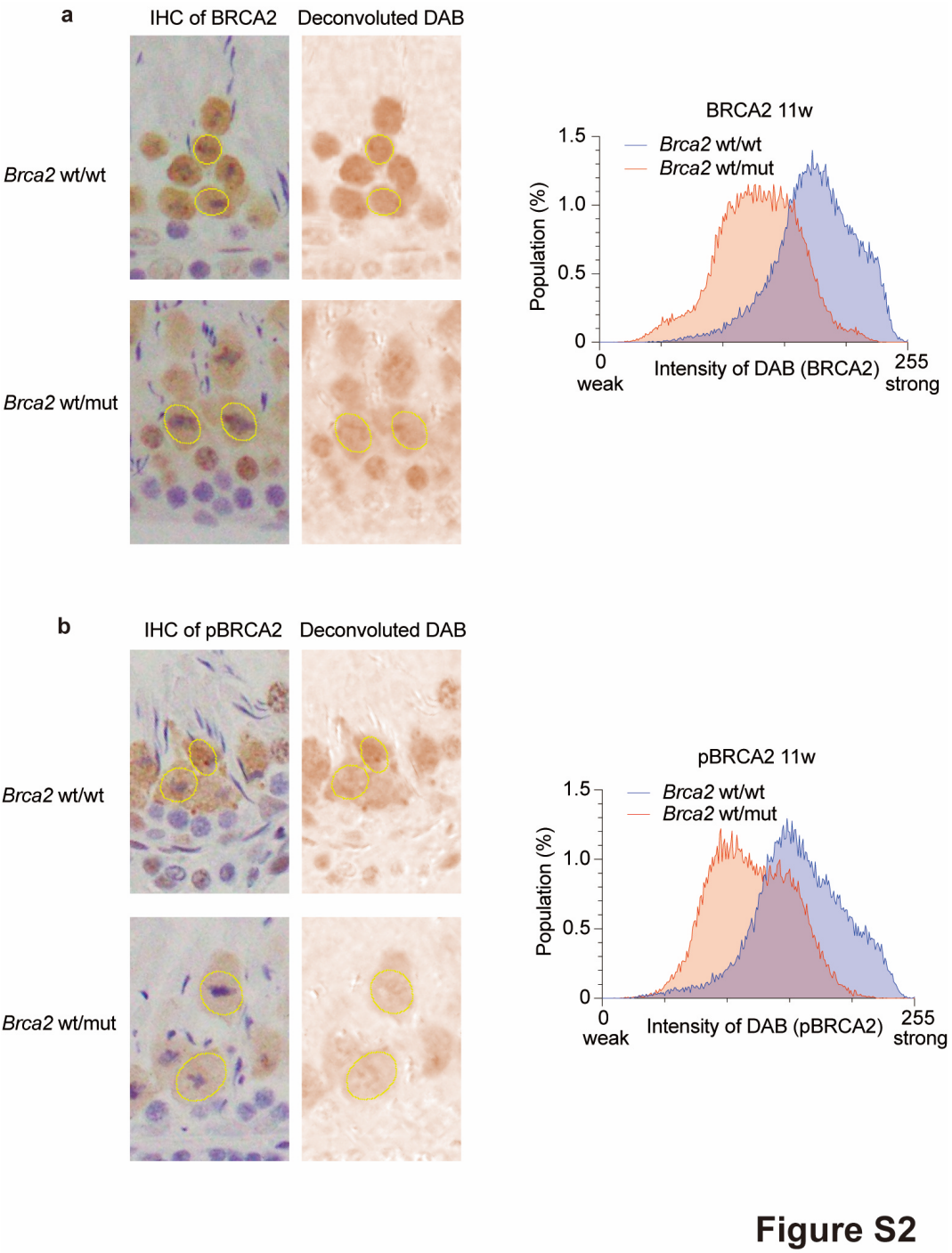

Figure S2

Figure S2. Metaphase spermatocytes in *Brca2*$^{wt/mut}$ testes exhibits lower staining intensity for BRCA2 and phosphorylated BRCA2 in immunohistochemistry compared to *Brca2*$^{wt/wt}$

(a, b) Typical microscopic imaged and staining intensity analysis of metaphase spermatocytes immunostained for (a) BRCA2 or (b) pBRCA2. In each case, 5 rats aged 11 weeks were evaluated. For each individual, 4-5 images were captured randomly at x20 magnification, ensuring inclusion of metaphase spermatocytes. From these images, five seminiferous tubules were selected , and two metaphase cells were chosen within circular ROIs (yellow circles). Subsequently, color deconvolution for DAB was performed, and staining intensity of DAB within each ROI was measured. Quantitative results from 10 metaphase spermatocytes per individual were summed to calculate the distribution of staining intensity. The average distribution ratio for each individual within the group is presented here. Both BRCA2 and pBRCA2 were stained weaker in *Brca2*$^{wt/mut}$ rats compared to *Brca2*$^{wt/wt}$. DAB: Diaminobenzidine; ROI: region of interest.

Figure S3. Uncropped images of membranes used for immunoblotting.

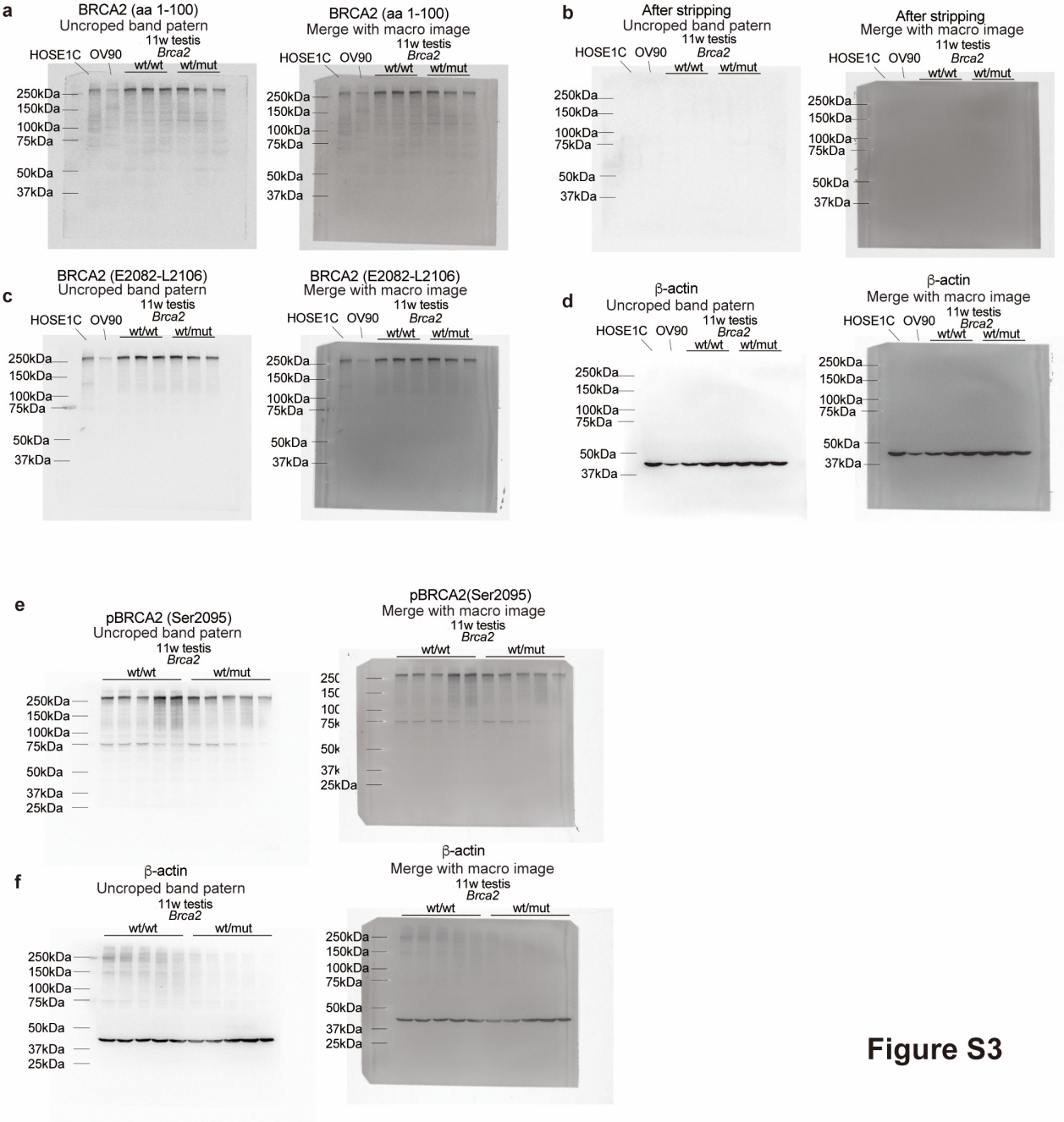

Figure S3

Figure S3. Uncropped images of membranes used for immunoblotting

(a-f) Uncropped band patterns and the figures merged with macroscopic images from immunoblotting analysis with antibodies against BRCA2 (aa 1-100), BRCA2 (E2082-L2106), phosphorylated BRCA2 (Ser2095),) and β-actin. Human cell lines, HOSE1C and OV90, lacking *BRCA2* mutations, are used for size reference. After evaluating BRCA2 (aa 1-100) (a), stripping was performed, and the removal of the antibody was confirmed to be enough (b). Subsequently, the same membrane was used to assess BRCA2 (E2082-L2106) and β-actin (c, d). Expression of BRCA2 and phosphorylated BRCA2 are slightly decreased in $Brca2^{wt/mut}$ testes without truncated or splicing variants.

92 **Figure S4. Immunohistochemistry shows no significant differences in oxidative stress**
93 **markers, 8-OHdG and 4-HNE, in the testes of Brca2wt/mut rat at 11 weeks**

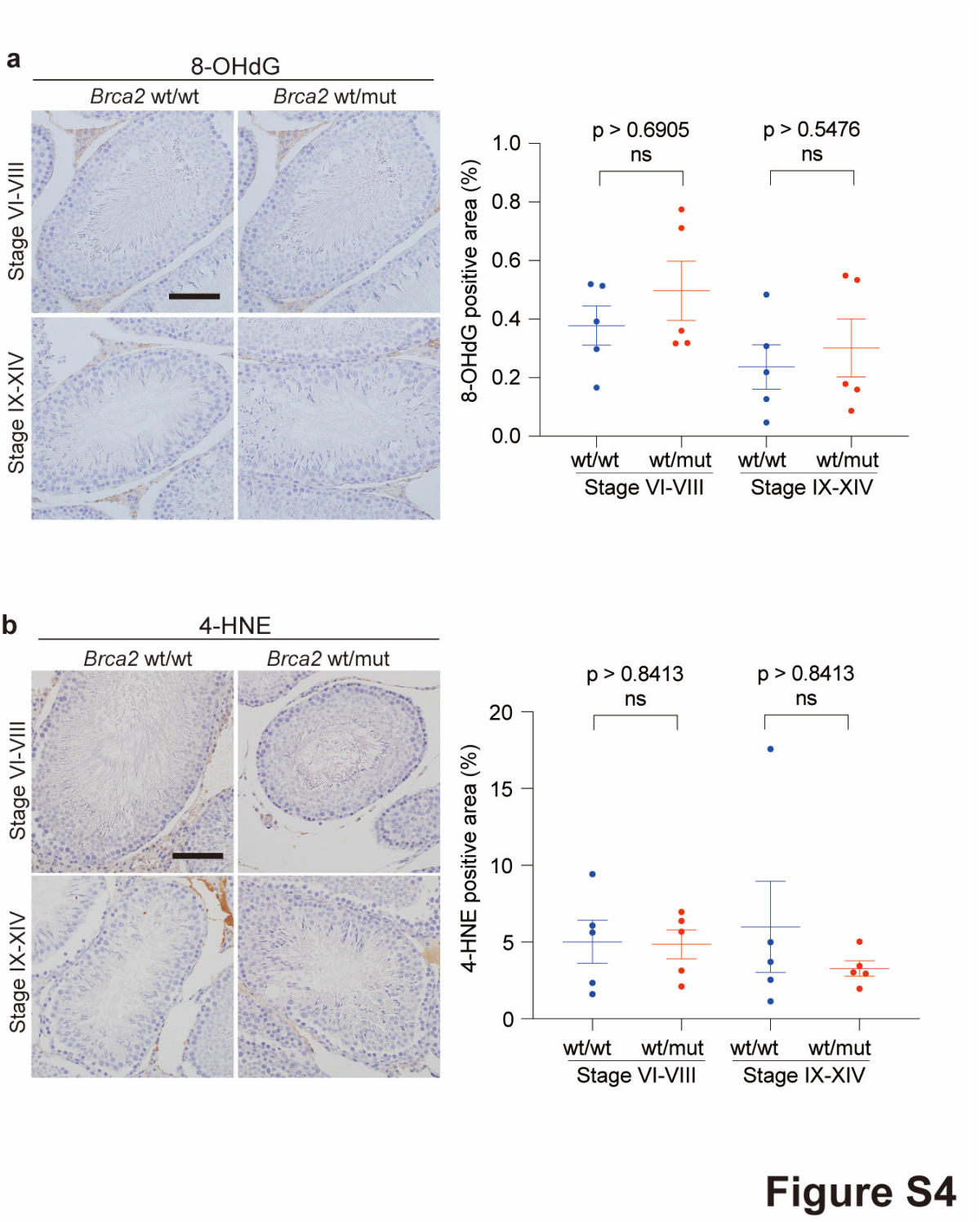

Figure S4

Figure S4. Immunohistochemistry shows no significant differences in oxidative stress markers, 8-OHdG and 4-HNE, in the testes of Brca2wt/mut rat at 11 weeks

(a, b) Representative immunostaining images of testes from 11-week-old rats using (a) 8-OHdG and (b) 4-HNE antibody, and quantitative analysis of these staining in spermatocytes within stage VI-VIII and stage IX-XIV seminiferous tubules (n = 5). These makers of oxidative stress exhibited no significant differences between *Brca2*$^{wt/wt}$ and *Brca2*$^{wt/mut}$ rats (bar = 100 μm).

Figure S5. Representative images of TUNEL staining for each main stage of seminiferous tubules

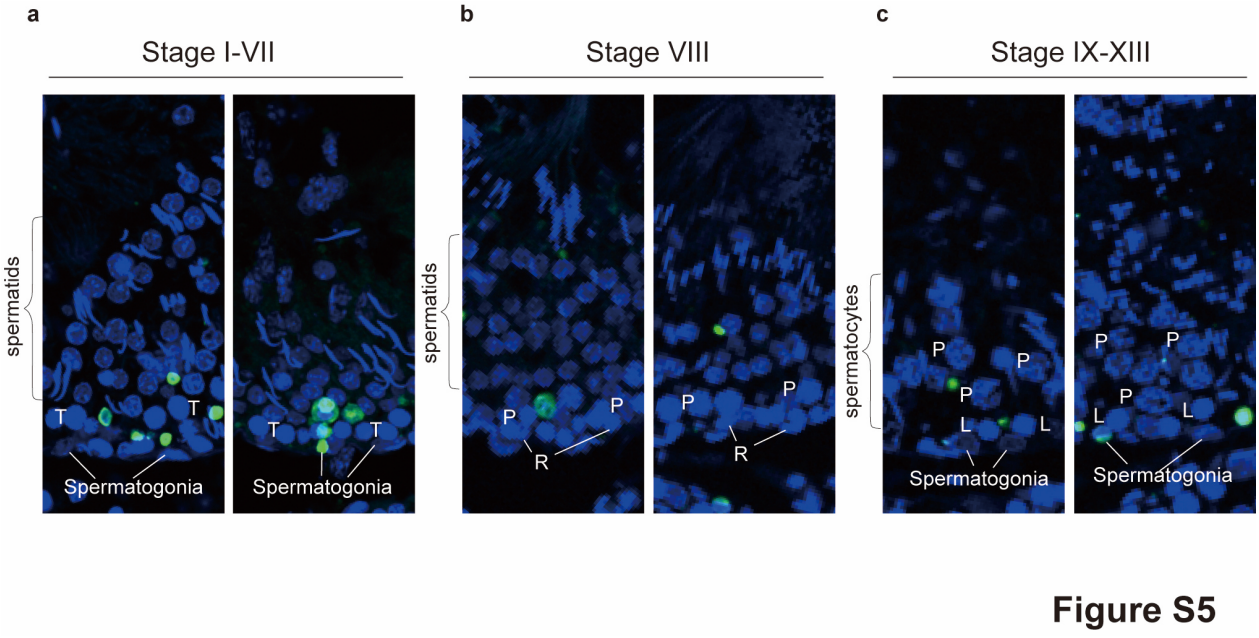

Figure S5. Representative images of TUNEL staining for each main stage of seminiferous tubules

(a-c) Typical images from TUNEL staining of seminiferous tubules from *BRCA2*$^{wt/mut.}$ rats. (a) In stage I-VII seminiferous tubules, spermatogonia with flat nuclei form a layer at the base, with a single layer of transition-form spermatocytes above them. Transition-form spermatocytes exhibit round nuclei, which are strongly stained by Hoechst 33342. Toward the luminal side, multiple layers of spermatids with small nuclei are observed. In the left image, transition-form spermatocytes and spermatid are TUNEL-positive whereas in the right image, spermatogonia, transition-form spermatocyte and spermatids are TUNEL-positive. (b) In stage VIII seminiferous tubules, spermatogonia with flat nuclei and resting spermatocytes with oval nuclei form a layer directory above the basement membrane. Toward the luminal side, a single layer of pachytene spermatocytes with round and slightly larger nuclei is distributed. Further toward the lumen, multiple layers of spermatids are observed. Here, in both images, spermatids are TUNEL-positive. (c) In stage IX-XIII seminiferous tubules, spermatogonia with flat nuclei are positioned on the basement membrane, with a single layer of leptotene spermatocytes located toward the lumen. Further toward the lumen, pachytene spermatocytes with enlarged nuclei are present in multiple layers, intermixed with small-nucleus spermatids. In the left image, leptotene and pachytene spermatocytes are TUNEL-positive whereas in right image, spermatogonia and leptotene spermatocytes are TUNEL-positive. R, resting spermatocytes; L, leptotene; T, transition form; P, pachytene.

129 **Figure S6. Representative plots of SCSA**

130

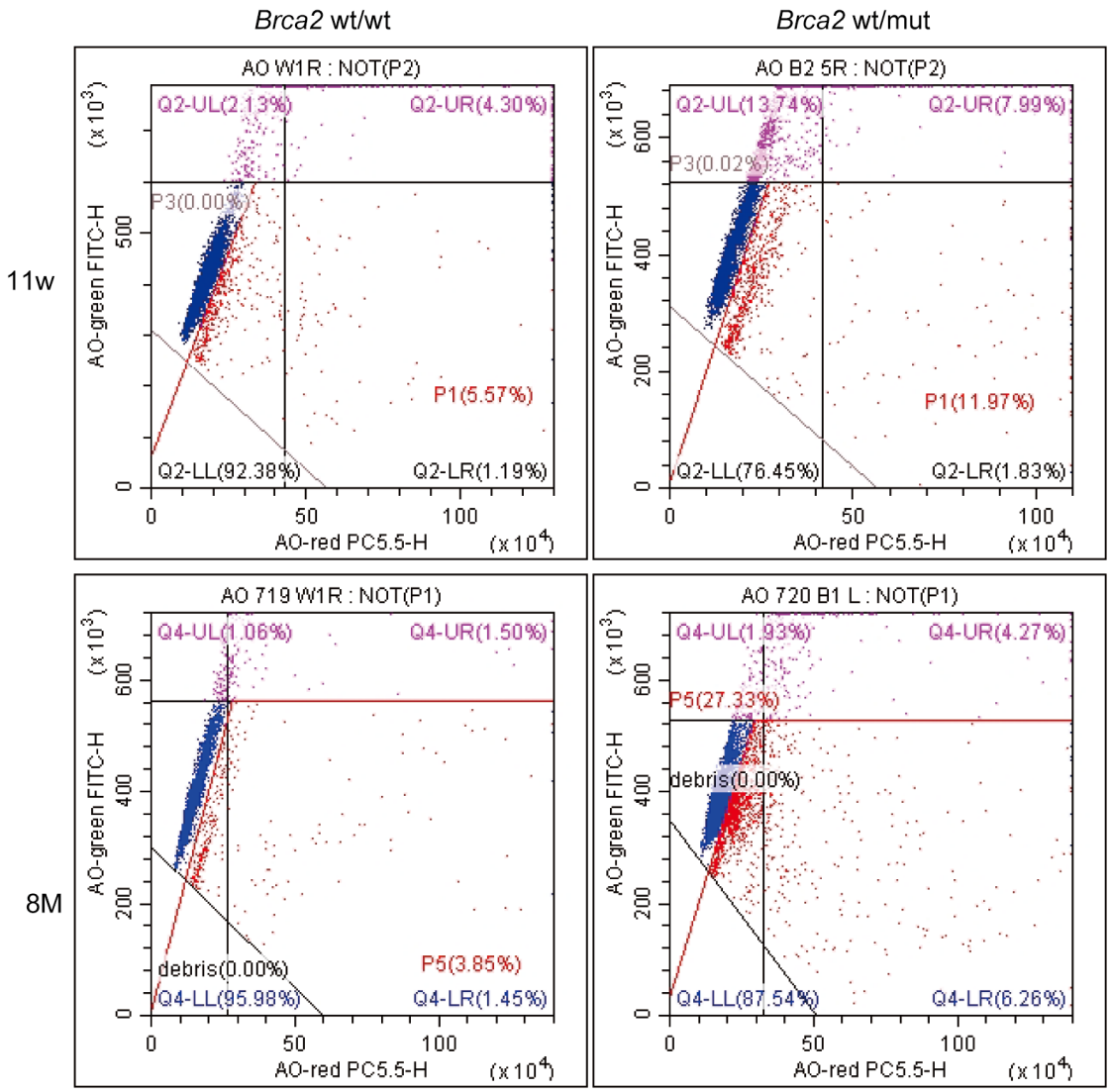

Figure S4

131

132

133

Figure S6. Representative plots of SCSA

Representative plots of SCSA performed on spermatozoa from *Brca2*$^{wt/wt}$ or *Brca2*$^{wt/mut}$ rats at the age of 11sweeks and 8 months. These plots indicate that spermatozoa from *Brca2*$^{wt/mut}$ contain a higher proportion of DNA fragmentation than those from *Brca2*$^{wt/wt}$ both at both 11 weeks and 8 months. In SCSA, the Acridine Orange (AO) equilibration buffer [400-µl acid detergent solution (0.08N HCl, 0.15M NaCl, 0.1% Triton X-100, pH 1.20) mixed with 1,200-µl AO staining solution (0.0006% AO, 0.1 M citric acid buffer, 0.2 M Na_2PO_4, DW)] was circulated in the flow cytometer's fluidic system for more than 15 min before evaluating the samples. Ten thousand events were recorded. The analysis was conducted in accordance with established protocols[56]. Briefly, AO-stained spermatozoa sample was inserted into the flow cytometer, in which the green and red fluorescence gains of the flow cytometer was adjusted so that the primary group of AO-green fluorescence nearly reaches the halfway up the Y-axis (green) whereas the AO-red fluorescence approximates 1/5 of the total X-axis (red). Then, gates were set up to identify spermatozoa with fragmented DNA, by drawing a horizontal gate along the top edge of the main cigar-shaped spermatozoa population, creating a straight gate on the right side of the cigar-shaped normal spermatozoa population, and making a 45-degree angled gate that intersects the lower boundary of the main cigar-shaped population to exclude apoptotic and dead spermatozoa along with other seminal debris. Spermatozoa with fragmented DNA are located in the area to the right of the main population, which includes the cigar-shaped plots. DNA fragmentation index (%DFI) was calculated via dividing the number of spermatozoa with fragmented DNA by the total number of spermatozoa. AO, Acridine Orange; SCSA, sperm chromatin structure assay; %DFI, % DNA fragmentation index.